

Evidence for a shared nuclear pore complex architecture that is conserved from the last common eukaryotic ancestor

Jeffrey A. DeGrasse,¹ Kelly N. DuBois,² Damien Devos,³ T. Nicolai Siegel,⁴ Andrej Sali,⁵ Mark C. Field,² Michael P. Rout,⁶ and Brian T. Chait^{1,*}

¹Laboratory of Mass Spectrometry and Gaseous Ion Chemistry, The Rockefeller University, 1230 York Ave, New York, NY 10065, USA, ²The Molteno Building, Department of Pathology, University of Cambridge, Tennis Court Road, Cambridge, CB2 1QP, UK, ³Structural Bioinformatics, European Molecular Biology Laboratory, Meyerhofstrasse 1, D-69117 Heidelberg, Germany, ⁴Laboratory of Molecular Parasitology, The Rockefeller University, 1230 York Ave, New York, NY 10065, USA, ⁵Department of Biopharmaceutical Sciences, University of California, San Francisco, 1700 4th Street, San Francisco, CA 94158, USA and ⁶Laboratory of Cellular and Structural Biology, The Rockefeller University, 1230 York Ave, New York, NY 10065, USA

*Correspondence to: chait@rockefeller.edu

Running head: Evolution of the nuclear pore complex

Keywords: evolution; transport mechanisms; nuclear pore complex; functional proteomics; biological mass spectrometry; structure prediction; *Trypanosoma brucei*

Abbreviations: FG Nup, phenylalanine-glycine nucleoporin; GFP, green fluorescent protein; Kap, karyopherin; LCEA, last common eukaryotic ancestor; NE, nuclear envelope; NPC, nuclear pore complex; Nup, nucleoporin; TbNEP, *Trypanosoma brucei* nuclear pore complex enriched preparation.

Summary

The nuclear pore complex (NPC) is a macromolecular assembly embedded within the nuclear envelope that mediates bidirectional exchange of material between the nucleus and cytoplasm. Our recent work on the yeast NPC has revealed a simple modularity in its architecture and suggested a common evolutionary origin of the NPC and vesicle coating complexes in a progenitor protoeukaryote. However, detailed compositional and structural information is currently only available for vertebrate and yeast NPCs, which are evolutionarily closely related. Hence, our understanding of NPC composition in a full evolutionary context is sparse. Moreover, despite the ubiquitous nature of the NPC, sequence searches in distant taxa have identified surprisingly few NPC components, suggesting that much of the NPC may not be conserved. Thus, in order to gain a broad perspective on the origins and evolution of the NPC, we performed proteomic analyses of NPC-containing fractions from a divergent eukaryote (*Trypanosoma brucei*) and obtained a comprehensive inventory of its nucleoporins. Strikingly, trypanosome nucleoporins clearly share with metazoa and yeast their fold type, domain organization, composition and modularity. Overall these data provide conclusive evidence that the majority of NPC architecture is indeed conserved throughout the eukaryota, and was already established in the last common eukaryotic ancestor. These findings strongly support the hypothesis that NPCs share a common ancestry with vesicle coating complexes, and that both were established very early in eukaryotic evolution.

Introduction

Nearly all eukaryotic cells possess an extensive endomembrane system that is principally responsible for protein targeting and modification (1). The nucleus, the defining eukaryotic feature, is separated from the cytoplasm by a double-bilayered nuclear envelope (NE) that is contiguous with the rest of this endomembrane system *via* connections to the endoplasmic reticulum. Nuclear pore complexes (NPCs) fenestrate the NE, serving as the exclusive sites mediating exchange between the nucleoplasmic and cytoplasmic compartments. Macromolecules are chaperoned through the NPC by numerous transport factors. It has been proposed that the endomembrane system and nucleus have an autogenous origin (i.e., evolving from invaginations of an ancestral plasma membrane) and was established early in eukaryotic evolution (2).

The composition of the NPC has been cataloged at ~30 distinct nucleoporins (Nups) (3) for the yeast *Saccharomyces cerevisiae* (4) and vertebrates (5), two members of the Opisthokonta (animals, fungi, and closely related protists). Ultrastructural studies have identified objects morphologically similar (at a first approximation) to opisthokont NPCs in the other major Eukaryote supergroups (6-8). However, very few data are available concerning the detailed NPC molecular composition and architecture for nearly all Eukaryotic lineages, leaving a relatively narrow view of the “typical” NPC and its origins. A few examples of potential Nup orthologs beyond the opisthokonts have been reported, leading to the suggestion that substantial portions of the NPC may have an ancient, pre-LCEA (last common eukaryotic ancestor) origin (9). However, a more extensive study has concluded that LCEA possessed a primitive ancestral NPC that passed few components to its modern descendants (10).

In yeast and vertebrates, the NPC consists of an eight-spoked core surrounding a central tube that serves as the conduit for macromolecular exchange. Each spoke can be divided into two similar nucleoplasmic and cytoplasmic halves. The eight spokes connect to form several coaxial rings: the membrane rings, the two outer rings at the nucleoplasmic and cytoplasmic periphery, and the two adjacent inner rings (11). Groups of Nups that we term “linker Nups” are attached between both sets of outer and inner rings. Another group of related proteins, collectively termed phenylalanine-glycine (FG) Nups, are largely exposed on the inner surface of the spokes and anchored either to the inner rings or to the linker Nups (11).

Opisthokont Nups can be grouped into three structural classes (11, 12). The first class comprises membrane-bound proteins that anchor the NPC into the NE. The second class is the core scaffold Nups; these proteins constitute the bulk of the NPC mass, form the central tube, and provide the scaffold for the deployment of the third class of Nups across both faces of the NPC. The core scaffold Nups are remarkably restricted at the structural level and contain only three distinct arrangements of two fold types: proteins dominated by an α -solenoid fold (also termed a helix-turn-helix repeat domain), proteins consisting of a β -propeller fold, and finally proteins composed of an amino-terminal β -propeller fold followed by a carboxy-terminal α -solenoid fold (which we here term a β - α structure) (12). FG Nups comprise the third class. These Nups carry multiply repeated degenerate “Phe-Gly” motifs (FG repeats), separated by hydrophilic or charged residues, which form large unstructured domains. Each FG Nup also contains a small structured domain (often a coiled-coil motif) that serves as the anchor site for interaction with the remainder of the NPC.

Many transport factors belong to a structurally related protein family collectively termed karyopherins (Kaps) (13, 14). Transport across the NPC depends on the interactions between Kaps, cargo molecules and the disordered repeat domains of FG Nups; the latter are thought to form the selective barrier for nucleocytoplasmic transport, guiding the Kap•cargo complexes (and other transport factors) through the central tube while excluding other macromolecules (reviewed in (3, 15-22)).

Significantly, we have previously noted that the fold composition and arrangement of many of the core scaffold Nups is shared with proteins that form coating structures that participate in the generation and transport of vesicles between different endomembrane compartments; significantly, many vesicle coating complex proteins and NPC scaffold Nups share an α -solenoid fold, β -propeller fold, or β - α structure (12, 23-28). These similarities gave rise to the “protocoatmer hypothesis”, which suggests a common ancestry for the NPC and these vesicle coat complexes. However, it is unclear how many, if any, of these particular core scaffold Nups are widely conserved, and hence it is unclear how general this potential relationship is throughout the eukaryota. Thus, two scenarios are possible. The first is that the coatmer-like proteins are only found in a subset of the eukaryotes (including the opisthokonts), indicating that they are a relatively recent acquisition of only some eukaryotes and are not a general feature of all NPCs. The second is that the coatmer-like proteins are conserved in all eukaryotes, providing strong support to the protocoatmer hypothesis. To directly address this issue we characterized the NPC of *Trypanosoma brucei*, a highly divergent but experimentally tractable organism, using proteomics. The resulting data indicate an ancient origin for the majority of the NPC components and shed light on the origin of LCEA itself.

Experimental procedures

Proteomic analysis of the Trypanosoma brucei nuclear pore complex enriched preparation (TbNEP): The overall strategy for the identification of the *T. brucei* Nups (TbNups) is depicted in Figure 1. The TbNEP was isolated as described (29). To reduce complexity and dynamic range within the sample and maximize the number of identifications, we employed five distinct fractionation strategies against the TbNEP (Figure 1 and Supplementary Data). These employed (i) SDS-PAGE with MALDI-MS (30, 31), (ii) hydroxyapatite chromatography fractionation prior to SDS-PAGE and MALDI-MS, (iii) binding TbNEP to a C4 cartridge, digestion with trypsin and analysis by LC-MS, (iv) differential enrichment of TbNEP proteins by chemical extraction prior to trypsin digestion and LC-MS (32) and (v) hydroxyapatite chromatography coupled to trypsin digestion and LC-MS. Peak lists were generated from the raw data using “Extract_msn” in Thermo Electron Xcalibur version 2.0 using default settings without enhancement or filters. The peak lists were submitted to X!Tandem (33) (version 2006.06.01.1) and searched against an in-house curated *T. brucei* protein database (generated July 5, 2005 using data from the genome sequencing project; the database was searched in its entirety). The X!Tandem search parameters were set as follows: missed cleavages permitted = 1; precursor ion tolerance = 4.0 Da; fragment ion tolerance = 0.4 Da; fixed modifications = carbamidomethylation of cysteine; variable modifications = oxidation of methionine. To reduce the possibility of false positives, only those individual MS/MS spectra with an expectation score better than 10^{-2} was considered.

Bioinformatic analysis of the TbNEP dataset: ORFs within the TbNEP dataset were queried against GeneDB to obtain annotations, functional assignments, structural information and sequence relationships to additional predicted gene products. ORFs were also analyzed and characterized by pair-wise sequence alignments (BLAST (34), PSI-BLAST, using three iterations (35) and FASTA (36)) against the National Center for Biotechnology Information (NCBI) non-redundant database and in-house nuclear envelope protein databases (primarily *Homo sapiens*, *Rattus norvegicus* and *S. cerevisiae* sequences). Unless otherwise noted, all algorithms were used with default search parameters. To search for the presence of conserved structural domains, a Hidden Markov Model (HMMer (37)) alignment to the Pfam HMM-profile database of domain families was conducted (38). Following the *in silico* analysis, functionally unassigned ORFs present within the TbNEP dataset were analyzed for several secondary structure elements, including β -sheets and α -helices (PSI-PRED (39)), transmembrane helices (Phobius (40)), natively unfolded regions (Disopred (41)) and coiled-coil regions (COILS (42)). Natively unfolded FG-repeat domains were identified using a pattern recognition algorithm developed in-house (PROWL, <http://prowl.rockefeller.edu>). Multiple sequence alignments were conducted with ClustalX (43). In some instances, multiple alignments were also subjected to phylogenetic analysis using MrBayes (44).

In situ tagging and visualization: Open reading frames of interest were *in situ* tagged using the pMOTag4G and pMOTag4H vectors (45); see supplementary data for details and primer sequences. The linear PCR products were purified and sterilized by ethanol precipitation. *T. brucei* Lister 427 procyclic stage cells were transfected by electroporation with 10-25 μ g of PCR product and cultured in SDM-79 (46, 47)

supplemented with 10% fetal bovine serum and 0.25% hemin. Following transfection, 25 $\mu\text{g/ml}$ of hygromycin was added and clones screened by limiting dilution. After three weeks at least three colonies were assayed for correct insertion and expression using PCR and/or Western blotting (Figure S1). For fluorescence microscopy tagged cell lines (suspended at 1×10^7 cells ml^{-1}) were fixed with 2% formaldehyde for 5 minutes at room temperature and allowed to settle onto a coverslip treated with (3-aminopropyl)triethoxy silane. Nonattached cells were washed away with phosphate buffered saline (PBS) and the coverslip was then mounted in 50% glycerol and 0.4 $\mu\text{g/ml}$ DAPI (4',6-diamino-2-phenylindole dihydrochloride) in PBS. Immunofluorescence microscopy was conducted similarly as above, except that after washing with PBS, the attached cells were permeabilized with 0.1% NP-40 in PBS. Subsequently, the coverslips were blocked for 20 minutes in PBG (PBS with 0.2% cold fish gelatin (Sigma) and 0.5% BSA) prior to incubation for 90 minutes with antibody (rabbit anti-Nup107, diluted to 1:100 (48)). After extensive washing with PBG, cells were incubated for 1 hour with TRITC-conjugated secondary antibody (mouse anti-rabbit, 1:500). Images were acquired either with the DeltaVision Image Restoration microscope (Applied Precision/Olympus) using an Olympus 100X/1.40NA objective or a Leica TCS-NT with a 63X/1.40NA objective. GFP was either imaged directly using FITC emission and excitation filters with a 2 second exposure or labeled, as above, with anti-GFP at 1:3000 (30) and then secondarily labeled with goat anti-rabbit IgG conjugated to Alexa 488, (Molecular Probes) at 1:1000. At least 15 Z-stacks (0.15 μm thickness) were acquired. Raw images were manipulated using a deconvolution algorithm (softWoRxTM v3.5.1, Applied Precision, enhanced

additive setting). Gamma levels and false colors were adjusted to enhance contrast only and final images assembled in Adobe Photoshop.

Results

Identification of putative *T. brucei* Nups: Sub-fractionation of *T. brucei* yields two fractions highly enriched in NPCs, namely an NE fraction and an NPC/lamina-enriched fraction (29). Here, we have performed a comprehensive proteomic analysis of these *T. brucei* nuclear pore complex enriched preparations (TbNEP) using multiple complementary approaches that identified a total of 757 proteins (Figure 1, Table 1, Table S1 and Supplementary Information). As anticipated, the high sequence divergence between eukaryote Nups precluded facile identification of orthologs based only on primary sequence comparisons (9, 10). Hence, we used a combination of experimental and *in silico* approaches to parse the TbNEP dataset. First, 448 proteins could be excluded on the basis that sequence homology searches clearly predicted a function that is unassociated with the TbNPC, such as ribosomal, endoplasmic reticulum and cytosolic proteins. The remaining 309 proteins were parsed for features associated with known Nups. These criteria were based on predicted fold types, the presence of sequence motifs, predicted molecular weight and predicted secondary structures. We employed a secondary structure prediction algorithm (PSIPred) to identify proteins with regions of predicted secondary structure consistent with the eight major fold types present within the vertebrate and yeast Nups (12). We also searched for motifs that are found within the NPC and NE, which include *trans*-membrane helices, natively unfolded regions (including those containing the FG repeats unique to nucleoporins), and coiled-coil regions (12). This filtered search is based on the hypothesis that the trypanosomatid NPC shares many architectural features with that of the opisthokonts, and would only miss those components that are species-specific or

too divergent to recognize. However, should this hypothesis prove incorrect, we would fail to identify the majority of the NPC components.

Using these approaches, we identified a total of 22 candidate trypanosome Nups (TbNups) (Table 1 and Supplementary Data). Each candidate TbNup was identified in at least two proteomic analyses, suggesting that this cohort represents enriched and relatively abundant proteins within the NPC-containing fractions, consistent with their assignment as candidate NPC-associated proteins. Five considerations suggest that we have identified most TbNups; (i) five ORFs in the *T. brucei* genome, Tb10.61.2630, Tb10.6k15.2350, Tb10.6k15.3670, Tb11.03.0140, and Tb927.4.5200, are annotated as putative TbNups based on sequence similarity; the products of all five ORFs were identified by our proteomic analysis, (ii) every recognizable FG repeat-containing polypeptide encoded by the trypanosome genome was detected in the proteome, (iii) eight transport factor homologs were identified, indicating that even transiently NPC-associated proteins are present in our preparations, (iv) we used proteomic strategies with progressively increasing dynamic ranges, allowing the identification of progressively less abundant proteins, the last of which more than doubled the total number of proteins in the dataset but identified no additional candidate TbNups (Figure 1) and (v) given the conserved morphology, size and symmetry of the trypanosome NPC (29), one would expect a similar number of trypanosome NPC components (22 identified nucleoporins) to that in yeast (30 nucleoporins, or 26 excluding yeast-specific gene duplications) and vertebrate (28 nucleoporins) (3). These criteria indicate that identification of NPC components within the TbNEP preparation was thorough, capturing the majority of the trypanosome nucleoporins.

Localization of *T. brucei* candidate nucleoporins: The candidate TbNups were localized by genomic-tagging and fluorescence microscopy (Table 1, Figures 2 and 3). Almost all the GFP-tagged candidate TbNups displayed a similar punctate decoration restricted to the rim of the nucleus (Figure 2). The punctae displayed a relatively homogeneous intensity and distribution; the average density of fluorescent punctae was 5.1 punctae/ μm^2 ($N = 10$, $\sigma = 0.8$), with an average of 93 punctae ($\sigma = 16$) per nucleus (see Figure 2A for an example). Such patterns are considered highly characteristic for Nups in all other eukaryotic taxa examined (49-53), and indeed all four of the annotated Nup homologs that we tested, Tb10.61.2630, Tb10.6k15.2350, Tb10.6k15.3670, and Tb11.03.0140, displayed this pattern. We confirmed using double labeling with a cross-reacting anti-Nup antibody that this pattern represents NPC localization (Figure 3A) (48). In total, 20 of the 22 putative TbNups displayed such punctate rim staining, identifying them as *bona fide* TbNups (Figure 2B). Multiple attempts to tag the two remaining candidate TbNups, Tb11.02.0270 and Tb927.4.5200, failed to generate positive clones. Seven additional proteins in the dataset are not classified as TbNups because they localized as diffuse or speckled staining in the cytosol or nucleus (Figure S2). Such localizations may be false negatives due to disrupted protein targeting upon C-terminal epitope tagging or alternatively may represent truly non-NPC-associated proteins.

Structural classification of TbNups

β -propeller and α -solenoid fold type containing TbNups: A well-conserved family of opisthokont Nups consist mainly of a β -propeller fold type (54). We find two clear examples in trypanosomes, Sec13p and also an ALADIN ortholog (TbNUP48). ALADIN

is also present in metazoa, plants but not *S. cerevisiae* (Figures 4 and S3A) (55). Significantly, a homolog of Seh1p, a β -propeller Nup in opisthokonts, is conspicuously absent from the proteome.

There are five *T. brucei* α -solenoid Nups (Figure 4); the number and mass of these proteins appear to have remained essentially unchanged between the Opisthokonta and trypanosomes. There are three smaller plus two larger α -solenoid Nups in *S. cerevisiae* (ScNup84, ScNup85, ScNic96; ScNup188, ScNup192), humans (HsNup107, HsNup75, HsNup93; HsNup188, HsNup205) and now trypanosomes (TbNup82, TbNup89, TbNup96; TbNup181, TbNup225). In most cases there is low sequence similarity between trypanosome, yeast, plant or human α -solenoid Nups (Figure S3B). For example, the nucleoporin interacting component (NIC) domain of ScNic96/HsNup93 is greatly diverged in trypanosomes and the Pfam expect values for alignment between the consensus NIC domain and trypanosome TbNup96 is 10^{-5} , compared to 10^{-177} (HsNup93) and 10^{-166} (ScNic96).

Proteins containing either β -propeller or α -solenoid fold types are ubiquitous (56). However, proteins with an N-terminal β -propeller fold and C-terminal α -solenoid fold (β - α structure) architecture are restricted to the endomembrane system and are important components of the coats in coated vesicles and the scaffold of the NPC (23). Trypanosomes have homologs (TbNup109 and TbNup132) for the two smaller β - α structure Nups of *S. cerevisiae* (ScNup120 and ScNup133) and humans (HsNup133 and HsNup160). There is also a larger β - α structure trypanosome Nup (TbNup144) that is orthologous to HsNup155 and the two *S. cerevisiae* HsNup155 paralogs (ScNup157, ScNup170) that arose from a yeast lineage specific genome-wide duplication (57). With

respect to primary structure, HsNup155, ScNup157, and ScNup170 are the only β - α structure Nups that are significantly conserved between opisthokonts and trypanosomes (Figure S3C).

A conserved β -sandwich domain: TbNup158 has a distinct and conserved domain structure. A highly conserved β -sandwich domain is situated between an FG repeat domain and an α -solenoid fold type (Figure 4), which unambiguously identifies this gene product as an ortholog of HsNup98-96 and ScNup145. In the opisthokonts, however, the β -sandwich domain displays an autoproteolytic activity that initiates self-cleavage at a conserved H[F/Y][S/T] tripeptide (58, 59). Although the β -sandwich domain is very highly conserved in *T. brucei* and the related excavate *Giardia lamblia*, both protist homologs lack the catalytic residues required for cleavage (Figure S5). Consistent with this finding, we found that the trypanosome homolog TbNup158 does not cleave and instead functions as the full-length protein, based on both Western blotting (Figure S1) and mass spectrometry.

FG repeat containing TbNups: Like their opisthokont counterparts, the FG regions of trypanosome FG Nups are predicted to be natively unfolded. An extraordinarily high rate of amino acid substitution within FG Nups (60, 61) results in huge sequence divergence (Table S2A), confounding *in silico* identification of homology. A high level of genomic plasticity may be a common feature among FG Nups. An example of such plasticity may be TbNup140 and TbNup149, which are encoded by adjacent genes with an abnormally small intergenic region; while Northern and Western blotting suggests two separately transcribed messages (Figures S1 and S9), in the related kinetoplastid *Leishmania major*, the ortholog LmjF28.3030 is apparently expressed as a single polypeptide. The

vertebrate, *S. cerevisiae* and trypanosome FG repeat domains generally have a similar frequency of F residues, approximately ~3-fold higher than the mean occurrence in their respective proteomes. Additionally, these domains are generally depleted in large side chain amino acids and enriched in small side chain residues. This compositional bias is likely a general feature for natively unfolded regions (60, 62). The abundance of G varies considerably between FG repeat domains, and displays a clear inverse correlation to the acidic and basic residues, D, E, R and K (Figures 5 and S4). Thus, Nup FG repeat domains generally fall into two groups; group I contain G enriched, DERK deficient sequences, and group II contain significantly less G than group A and substantially more DERK residues (Figure 5). Among the FG Nups, the homologs of TbNup158 can be uniquely identified due to the characteristic nature of their characteristic domains (see above). It is noteworthy that the FG regions of all the homologs of TbNup158 fall into group I, suggesting that the function of a given FG domain is conserved even if its sequence is not. In yeast and vertebrates, FG Nups that are symmetrically localized tend to fall into group I, while Nups with an asymmetric localization fall into group II, albeit with some exceptions. While the locations of these trypanosome Nups are currently not known, it will be of significant interest to ascertain if this compositional feature is a potential predictor for FG Nup location. There is also some conservation in the structured domains of the FG Nups; TbNup53a, TbNup53b, TbNup59, and TbNup62 all possess a putative coiled-coil domain, which - as it does in their yeast and vertebrate counterparts - likely serves to anchor these Nups to the NPC (Figure 4) (12).

Nuclear basket: Two members of the validated TbNup cohort, TbNup110 and TbNup92, exhibited highly characteristic localizations distinct from the other TbNups. Both partially co-localize with the NPCs (Figure 3A) but are also found between NPCs at the inner face of the NE. Both proteins also have large predicted coiled-coil domains (Table 1). Their location and domain architecture are highly reminiscent of metazoan Tpr and its homologs *S. cerevisiae* Mlp1p/Mlp2p and *Schizosaccharomyces pombe* Nup211p and Alm1p (although at the sequence level they have undergone extensive species-specific divergence or may not share common ancestry) (Figures 4 and S3D). These proteins appear to be components of the nuclear basket (63-68). Significantly, while TbNup110 maintains a NPC location throughout the cell cycle, TbNup92 relocalizes during late mitosis to NE regions opposite the division plane, where the mitotic spindle is likely anchored (Figure 3B) (69). Localization to the spindle pole body is observed for one each of the *S. pombe* and *S. cerevisiae* Tpr homologs, Alm1p and Mlp2p respectively, remarkably similar in behavior to TbNup92. This suggests, together with the structural data, that TbNup92 is an Mlp2 analogue (64, 65) and that TbNup92 and TbNup110 are components of the basket structure at the trypanosome NPC nuclear face (29).

Integral membrane proteins: The membrane trypanosome Nups remain unidentified. Of the unannotated proteins within the TbNEP, 30% are predicted to contain at least one *trans*-membrane helix (Table S1) but none contain a domain structure characteristic of opisthokont membrane Nups (i.e. cadherin-like domains for Pom152 or gp210, or NE constituents). One possibility is that we have failed to recognize the integral membrane

Nups; given the extremely low similarity between yeast and vertebrate membrane Nups this would not be surprising.

Transport factors: In addition to 22 TbNups, we identified 9 transport factors in the proteome (Table 1). These proteins generally prove easier to identify by sequence homology searches than the TbNups because of a relatively high sequence similarity retained across the Eukaryota (Figure S6). This sequence conservation is possibly due to the large number of interactions that these molecules must support, although additional factors may also be important.

Divergent features of the TbNPC: The TbNEP did not contain any obvious homologs for several Nups found in *S. cerevisiae* or vertebrates. These include HsNup358, ScNup2, HsNup214/ScNup159, Seh1 and HsNup88/ScNup82. It is unlikely that these proteins have been overlooked as all have readily observable fold type, domain and motif signatures, e.g. HsNup88/ScNup82 contains a β -propeller fold. It is therefore likely that these Nups have been either lost or diverged such that even *in silico* domain prediction fails. The presence of homologs of these Nups, as well as any trypanosomatid-specific Nups, will be elucidated with further investigations – potentially by co-immunoprecipitation or similar strategies.

Modular duplications in the NPC: Each of the *S. cerevisiae* NPC spokes can be divided into two columns, in which almost every Nup in one column has a counterpart of similar size, fold and position in the adjacent column, and it is almost certain this holds true for the vertebrate NPC as well (11). We show here that this relationship also extends to trypanosomes (Figure S8), indicating that an underlying 16-fold symmetry is

likely universal. We previously proposed that a simpler module underwent ancient duplication and divergence events to generate the current NPC (11). The folds and orthologous relationships detected for trypanosomes (Figure S8) fully support this modular duplication, which must have occurred prior to LCEA.

Discussion

During the transition from prokaryote to eukaryote, cells gained a cytoskeleton, an elaborate endomembrane system and a nucleus. The order in which these events occurred has been challenging to infer; there is no primitive state among extant eukaryotes (69, 70) and any reconstruction of evolutionary history has relied on the assumption that all modern eukaryotes derived from a LCEA. Because the NPC, a nuclear component in all eukaryotes, functions to maintain the distinct compositions of the nucleoplasm and cytoplasm, it is likely that the NPC co-evolved with the nuclear envelope. The NPC also retains distant relationships to intracellular transport systems (11, 12, 23).

Degree of conservation of the NPC among eukaryotes: We believe that we have identified the majority of the trypanosome nucleoporins (see Results), certainly enough to permit meaningful comparisons with the nucleoporin composition of opisthokont NPCs. Thus, by comparing validated sets of trypanosome and opisthokont Nups we are able to access the degree of conservation of NPC architecture across the Eukaryota, providing insight into both the LCEA and relationships between the NPC and endomembrane trafficking factors. Significantly, trypanosome NPC components share a

remarkable level of architectural and compositional complexity with opisthokont Nups. Moreover, except for the *trans*-membrane domain Nups which remain cryptic, homologs of all major classes of NPC proteins could be identified, despite great levels of sequence divergence. Rather than primary structures, eukaryotes appear to preserve the detailed fold arrangements within their NPC components.

This high level of conservation indicates an ancient origin for much of the NPC's structure. The opisthokont NPC core scaffold is comprised almost entirely of β -propeller and α -solenoid fold types (11, 71). Eleven TbNups contain these folds, representing a remarkable degree of concordance between number, molecular weight and architecture when compared against opisthokont core scaffold counterparts (Figures 4 and S8). Given the evolutionary distance between these lineages, this concordance strongly suggests a near-universal conservation of the basic NPC architecture. Further, although the sequences of trypanosome FG Nups are highly divergent compared to opisthokonts, they all share: (i) extensive regions bearing F repeats, (ii) flanking of F by a small amino acid, usually G, and (iii) composition of the spacer residues, particularly in respect to charge. These highly conserved features also point to a conserved mechanism for mediating nucleocytoplasmic transport (72).

A further conserved NPC component appears to be the nuclear basket (29, 49, 73). Two putative *T. brucei* basket components, TbNup92 and TbNup110, consist of coiled-coiled domains and localize to the NPC, but present negligible sequence similarity to ScMlp1p, ScMlp2p or HsTpr. Furthermore, TbNup92 and TbNup110 are clearly nonparalogous, unlike ScMlp1p and ScMlp2p. However, similar to ScMlp1, TbNup110 localizes to the NPC throughout the cell cycle while TbNup92 localizes to a position

proximal to the spindle pole during mitosis, analogous to ScMlp2 (67). *S. pombe* possesses a similar configuration to trypanosomes; two Mlp analogs, of which only one exhibits differential localization during mitosis (64, 65). Only one such protein, Tpr, is present in metazoa. Our data do not allow unequivocal assignment of TbNup92 and TbNup110 as nuclear basket proteins, but a trypanosome nuclear basket has been visualized (29) and the overall architecture and behavior during mitosis of these proteins is highly suggestive of analogous function and hence location. If TbNup92 and TbNup110 are indeed components of the trypanosome nuclear basket this would indicate that basket proteins share essentially no sequence similarity, and are potentially the products of lineage-specific gene duplications. These duplications may represent an instance of convergent evolution. Retention of the basket structure itself, however, would point to its importance in the overall mechanism of nuclear transport, likely at the level of RNA export (3).

Despite conservation of the NPC, homologs of membrane-bound Nups were not identified. It seems unlikely that such proteins were depleted from the TbNEP, as we readily identified a great many *trans*-membrane domain-containing proteins within this material. This may imply that while both the core and FG Nups are conserved, membrane-associated Nups are unrecognizable by our algorithms. Alternatively, the fact that pore membrane proteins are apparently dispensable for NPC function and assembly in *Aspergillus* (74) might indicate that membrane proteins are not a necessary component of the trypanosome NPC. Similarly, prominent peripheral opisthokont Nups are also absent from our proteome; again, these may be unidentified, truly absent or replaced by trypanosome-specific analogues. Finally, vertebrates carry three additional

β -propeller Nups when compared with *S. cerevisiae*. Two possibilities could account for this; their ancestor had a simpler NPC which was elaborated in vertebrates, or yeast lost these proteins (75). The presence of one of these additional β -propeller domain Nups (ALADIN) in trypanosomes clearly favors the secondary loss model.

The protocoatmer hypothesis for the origin of NPC and coated vesicles: The similarity between the core scaffold Nups and components of vesicle coatmer complexes in both yeast and metazoa led to the suggestion that a pre-LCEA primitive membrane deforming complex evolved into both the NPC and the diverse set of membrane coat systems in extant Eukaryotic taxa (11, 12, 23). Significantly, if general membrane deforming complexes were the first components to arise, the model would then suggest that the basic α -solenoid/ β -propeller architecture pre-dates emergence of the NPC/NE (23). A key test of this “protocoatmer hypothesis” is therefore that these structural features must be retained by the contemporary NPC of all eukaryotes; however, prior *in silico* analysis has failed to provide unequivocal evidence (10).

The presence of an extensive trypanosome repertoire of β -propeller, α -solenoid, and β - α structure proteins, all abundant in vesicle-coating complexes and restricted to the eukaryotic endomembrane system, plus clear conservation of a large proportion of the opisthokont NPC core by the trypanosome NPC, strongly supports the protocoatmer hypothesis for the origin of eukaryotic endomembrane systems (12, 23). Evidence in favor includes: the similar inventory, predicted molecular weight and domain structure of the core Nups; the similar number and conserved amino acid composition of the FG Nups; the markedly similar morphology of NPCs across the Eukaryota; conservation of soluble transport factors, which suggests a conserved nuclear transport mechanism;

and detectable sequence similarity between a minority of trypanosome and opisthokont Nups, including the highly conserved β -sandwich autoproteolytic domain of TbNup158 (Supplementary Data). Others have suggested that LCEA possessed an ancestral NPC with little resemblance to the modern one, passing few components to its descendants (10). However, the evidence here leads us to reject this model, and instead robustly supports a model positing a common origin from a complex NPC followed by extensive divergent evolution (Figure 6). It therefore follows that the LCEA likely possessed an NPC that was structurally analogous to the contemporary NPCs found in extant taxa, revealing its ancient relationship with vesicle coating complexes.

Acknowledgements: The authors wish to acknowledge members of the B.T. Chait, M.P. Rout and G.A.M. Cross laboratories for their assistance and discussions. We thank Alison North and the R.U. BIRC for invaluable help with imaging. Numerous colleagues, including J.B. Dacks, J.S. Glavy, D. Fenyő, M. Niepel, J.C. Padovan, and B. Ueberheide have offered assistance and discussion, to which the authors are indebted. This work was supported by grants from the US National Institutes of Health to B.T.C. (RR00862), M.P.R. (GM062427), M.P.R. and B.T.C. (RR022220), a Tri-Institutional Training Program in Chemical Biology to J.A.D. and a Wellcome Trust Grant (082813/Z/07/Z) to M.C.F. and M.P.R.

References

1. Dacks JB & Field MC (2007) *J Cell Sci* **120**, 2977-2985.
2. Cavalier-Smith T (1975) *Nature* **256**, 463-468.

3. Suntharalingam M & Wenthe SR (2003) *Developmental Cell* **4**, 775-789.
4. Rout MP, Aitchison JD, Suprpto A, Hjertaas K, Zhao YM, & Chait BT (2000) *J Cell Biol* **148**, 635-651.
5. Cronshaw JA, Krutchinsky AN, Zhang WZ, Chait BT, & Matunis MJ (2002) *J Cell Biol* **158**, 915-927.
6. Akey CW & Radermacher M (1993) *J Cell Biol* **122**, 1-19.
7. Lim RYH, Aebi U, & Stoffler D (2006) *Chromosoma* **115**, 15-26.
8. Lim RYH & Fahrenkrog B (2006) *Current Opinion in Cell Biology* **18**, 342-347.
9. Baptiste E, Charlebois RL, Macleod D, & Brochier C (2005) *Genome Biology* **6**.
10. Mans BJ, Anantharaman V, Aravind L, & Koonin EV (2004) *Cell Cycle* **3**, 1612-1637.
11. Alber F, Dokudovskaya S, Veenhoff LM, Zhang W, Kipper J, Devos D, Suprpto A, Karni-Schmidt O, Williams R, Chait BT, *et al.* (2007) *Nature* **450**, 695.
12. Devos D, Dokudovskaya S, Williams R, Alber F, Eswar N, Chait BT, Rout MP, & Sali A (2006) *Proceedings of the National Academy of Sciences of the United States of America* **103**, 2172-2177.
13. Moroianu J, Blobel G, & Radu A (1995) *Proceedings of the National Academy of Sciences of the United States of America* **92**, 2008-2011.
14. Radu A, Blobel G, & Moore MS (1995) *Proceedings of the National Academy of Sciences of the United States of America* **92**, 1769-1773.
15. Pemberton LF & Paschal BM (2005) *Traffic* **6**, 187-198.
16. Becskei A & Mattaj LW (2005) *Current Opinion in Cell Biology* **17**, 27-34.
17. Macara IG (2001) *Microbiol. Mol. Biol. Rev.* **65**, 570-+.

18. Peters R (2005) *Traffic* **6**, 421-427.
19. Quimby BB & Dasso M (2003) *Current Opinion in Cell Biology* **15**, 338-344.
20. Rout M, Aitchison J, Suprpto A, Hjertaas K, Zhao YM, & Chait B (2001) *Faseb J* **15**, A864-A864.
21. Rout MP & Aitchison JD (2001) *Journal of Biological Chemistry* **276**, 16593-16596.
22. Weis K (2003) *Cell* **112**, 441-451.
23. Devos D, Dokudovskaya S, Alber F, Williams R, Chait BT, Sali A, & Rout MP (2004) *PLoS Biology* **2**, e380.
24. Dokudovskaya S, Williams R, Devos D, Sali A, Chait BT, & Rout MP (2006) **14**, 653-660.
25. Debler EW, Ma Y, Seo H-S, Hsia K-C, Noriega TR, Blobel G, & Hoelz A (2008) **32**, 815-826.
26. Hsia K-C, Stavropoulos P, Blobel G, & Hoelz A (2007) **131**, 1313-1326.
27. Boehmer T, Jeudy S, Berke IC, & Schwartz TU (2008) **30**, 721-731.
28. Schrader N, Koerner C, Koessmeier K, Bangert J-A, Wittinghofer A, Stoll R, & Vetter IR (2008) **16**, 1116-1125.
29. Rout MP & Field MC (2001) *Journal of Biological Chemistry* **276**, 38261-38271.
30. Cristea IM, Williams R, Chait BT, & Rout MP (2005) *Molecular & Cellular Proteomics* **4**, 1933-1941.
31. Tackett AJ, Dilworth DJ, Davey MJ, O'Donnell M, Aitchison JD, Rout MP, & Chait BT (2005) *J Cell Biol* **169**, 35-47.

32. Schirmer EC, Florens L, Guan TL, Yates JR, & Gerace L (2003) *Science* **301**, 1380-1382.
33. Craig R & Beavis RC (2004) *Bioinformatics* **20**, 1466-1467.
34. Altschul SF, Gish W, Miller W, Myers EW, & Lipman DJ (1990) *Journal of Molecular Biology* **215**, 403-410.
35. Altschul SF, Madden TL, Schaffer AA, Zhang JH, Zhang Z, Miller W, & Lipman DJ (1997) *Nucleic Acids Research* **25**, 3389-3402.
36. Pearson WR & Lipman DJ (1988) *Proceedings of the National Academy of Sciences of the United States of America* **85**, 2444-2448.
37. Eddy SR (1998) *Bioinformatics* **14**, 755-763.
38. Sonnhammer ELL, Eddy SR, Birney E, Bateman A, & Durbin R (1998) *Nucleic Acids Research* **26**, 320-322.
39. McGuffin LJ, Bryson K, & Jones DT (2000) *Bioinformatics* **16**, 404-405.
40. Kall L, Krogh A, & Sonnhammer ELL (2004) *Journal of Molecular Biology* **338**, 1027-1036.
41. Ward JJ, Sodhi JS, McGuffin LJ, Buxton BF, & Jones DT (2004) *Journal of Molecular Biology* **337**, 635-645.
42. Lupas A, Vandyke M, & Stock J (1991) *Science* **252**, 1162-1164.
43. Thompson JD, Gibson TJ, Plewniak F, Jeanmougin F, & Higgins DG (1997) *Nucleic Acids Research* **25**, 4876-4882.
44. Huelsenbeck JP & Ronquist F (2001) *Bioinformatics* **17**, 754-755.
45. Oberholzer M, Morand S, Kunz S, & Seebeck T (2006) *Molecular and Biochemical Parasitology* **145**, 117-120.

46. Brun R & Schonenberger M (1979) *Acta Tropica* **36**, 289-292.
47. Field MC, Horn D, & Carrington M (2008) in *Small Gtpases in Disease, Part A*, pp. 57-76.
48. Glavy JS, Krutchinsky AN, Cristea IM, Berke IC, Boehmer T, Blobel G, & Chait BT (2007) *Proceedings of the National Academy of Sciences of the United States of America* **104**, 3811-3816.
49. Beck M, Forster F, Ecke M, Plitzko JM, Melchior F, Gerisch G, Baumeister W, & Medalia O (2004) *Science* **306**, 1387-1390.
50. Davis LI & Blobel G (1986) *Cell* **45**, 699-709.
51. Davis LI & Fink GR (1990) *Cell* **61**, 965-978.
52. De Souza CPC, Horn KP, Masker K, & Osmani SA (2003) *Genetics* **165**, 1071-1081.
53. Whalen WA, Yoon JH, Shen RL, & Dhar R (1999) *Genetics* **152**, 827-838.
54. Siniosoglou S, Wimmer C, Rieger M, Doye V, Tekotte H, Weise C, Emig S, Segref A, & Hurt EC (1996) *Cell* **84**, 265-275.
55. Cronshaw JM & Matunis MJ (2003) *Proceedings of the National Academy of Sciences of the United States of America* **100**, 5823-5827.
56. Andrade MA, Perez-Iratxeta C, & Ponting CP (2001) *Journal of Structural Biology* **134**, 117-131.
57. Wolfe KH & Shields DC (1997) *Nature* **387**, 708-713.
58. Fontoura BMA, Blobel G, & Matunis MJ (1999) *J Cell Biol* **144**, 1097-1112.
59. Rosenblum JS & Blobel G (1999) *Proceedings of the National Academy of Sciences of the United States of America* **96**, 11370-11375.

60. Denning DP, Patel SS, Uversky V, Fink AL, & Rexach M (2003) *Proceedings of the National Academy of Sciences of the United States of America* **100**, 2450-2455.
61. Denning DP & Rexach MF (2007) *Molecular & Cellular Proteomics* **6**, 272-282.
62. Weathers EA, Paulaitis ME, Woolf TB, & Hoh JH (2004) *Febs Letters* **576**, 348-352.
63. Byrd DA, Sweet DJ, Pante N, Konstantinov KN, Guan TL, Saphire ACS, Mitchell PJ, Cooper CS, Aebi U, & Gerace L (1994) *J Cell Biol* **127**, 1515-1526.
64. Chen XQ, Du XM, Liu JH, Balasubramanian MK, & Balasundaram D (2004) *Yeast* **21**, 495-509.
65. Jimenez M, Petit T, Gancedo C, & Goday C (2000) *Molecular And General Genetics* **262**, 921-930.
66. Krull S, Thyberg J, Bjorkroth B, Rackwitz HR, & Cordes VC (2004) *Molecular Biology of the Cell* **15**, 4261-4277.
67. Niepel M, Strambio-de-Castillia C, Fasolo J, Chait BT, & Rout MP (2005) *J Cell Biol* **170**, 225-235.
68. Strambio-de-Castillia C, Blobel G, & Rout MP (1999) *J Cell Biol* **144**, 839-855.
69. Adl SM, Simpson AGB, Farmer MA, Andersen RA, Anderson OR, Barta JR, Bowser SS, Brugerolle G, Fensome RA, Fredericq S, *et al.* (2005) *Journal of Eukaryotic Microbiology* **52**, 399-451.
70. Dacks JB, Walker G, & Field MC (2008) *Parasitology International* **57**, 97-104.
71. Alber F, Dokudovskaya S, Veenhoff LM, Zhang WZ, Kipper J, Devos D, Suprpto A, Karni-Schmidt O, Williams R, Chait BT, *et al.* (2007) *Nature* **450**, 683-694.

72. Rexach M & Blobel G (1995) *Cell* **83**, 683-692.
73. Kiseleva E, Goldberg MW, Daneholt B, & Allen TD (1996) *Journal of Molecular Biology* **260**, 304-311.
74. Liu H-L, De Souza CPC, Osmani AH, & Osmani SA (2008) *Mol. Biol. Cell*, E08-06-0628.
75. Yang Q, Rout MP, & Akey CW (1998) *Mol. Cell.* **1**, 223-234.

Figure legends

Figure 1. Summary flowchart of biochemical, mass spectrometric, and bioinformatic methods used to identify putative *T. brucei* nucleoporins and transport factors. Strategies 1-5 are indicated by the red, blue, green, purple and black colored arrows, respectively. The boxes are colored as follows: gold, protein recovery steps; light blue, protein separation steps; and, brown, mass spectrometry techniques. Following mass spectrometry, the bioinformatic strategy outlined here identified 30 putative TbNPC associated proteins from the initial pool of 757 identified proteins in the TbNEP. SDS-PAGE of fractions from a representative hydroxyapatite separation of the nuclear envelope fraction is shown at top left. FW, flowthrough and wash. Concentrations of phosphate in the elution buffer are indicated above the gel lanes, and apparent molecular weights (in kDa) are shown to the left of the gel. SDS-PAGE of *T. brucei* NE proteins that have been subjected to chemical extraction is shown at top right. The three extractions (base, salt and detergent, and heparin) are separated by vertical dashed lines. The pellet (P) and supernatant (S) are indicated. The number of Nups versus the total number of proteins identified with each successive strategy is depicted in the scatter plot (bottom right). Although, the total number of proteins identified increases dramatically with further experimentation, the number of NPC-associated proteins levels off after four strategies.

Figure 2: Validation of candidate *T. brucei* Nups. (A) One copy of open reading frame Tb11.03.0140 (TbNup158) was genomically tagged at the COOH-terminus with GFP. A montage of 21 confocal planes from the analysis of a TbNup158-tagged

trypanosome in late anaphase is shown; each z-slice is 150nm thick. There are ~150 punctae associated with the nuclear envelope in this example. (B) Fluorescent microscopy gallery of COOH-terminal genomically-labeled TbNups and corresponding DAPI fluorescence to visualize the DNA. Apart from TbSec13, which was labeled using the 3xHA epitope and visualized with a mouse monoclonal anti-HA antibody at 1:1000, all other open reading frames were tagged with GFP. Scale bars, 2 μ m.

Figure 3: TbNup92 exhibits cell-cycle dependent localization. (A) A rabbit polyclonal antibody against HsNup107 (35) was used to stain a trypanosome cell bearing tagged TbNup89. Colocalization of these signals further supports assignment of the punctae as the trypanosome NPC (top). Two coiled-coil TbNups, TbNup110 and TbNup92, only partially co-localize with this antibody, and are found immediately to the nuclear side of the NPCs and adjacent to them, suggesting association with the nuclear basket of the NPC, and consistent with potential similarity to Tpr (bottom). (B) TbNup110-GFP and TbNup92-GFP, visualized in mitotic cells, demonstrates that while TbNup110 remains associated with the NPC throughout mitosis, TbNup92 relocates to opposite poles, in a similar region to the spindle attachment site. Scale bar, 2 μ m.

Figure 4: Predicted secondary structure features, fold and location for validated TbNups. The ruler at top indicates residue number. Within a map, the horizontal black line represents the polypeptide length of the Nup with the NH₂-terminus to the left. The y-axis indicates the confidence score of the predicted secondary structure element.

Predicted α -helices are shaded in magenta, predicted β -sheets are in blue, and predicted coiled-coil regions are in red. The vertical orange lines below the primary structure indicate FG dipeptides. Representative models of the Nup domains, colored according to their fold type, are shown to the left. The TbNups are binned according to their predicted fold type, and thus probable function, within the TbNPC; possible yeast and human homologs are indicated in the right-most column. Predicted positions of each Nup or Nup structural class within the NPC are shown at right, based on the architecture as determined for *S. cerevisiae*.

Figure 5: Correlation between the frequency of glycine and charged residues in trypanosome, yeast, and human FG repeat Nups. The percent composition of Gly is plotted against Asp, Glu, Arg, and Lys (DERK) residue frequency. Each data point represents an FG Nup from either *S. cerevisiae* (blue), *H. sapiens* (red), or a candidate FG Nup from *T. brucei* (green). The diameter of each data point is directly proportional to the phenylalanine concentration within the respective Nup. FG Nups tend to cluster into two groups: high Gly, low DERK (Group I) and low Gly, high DERK (Group II). The average natural occurrence (in vertebrates) for Phe is ~4%, for Gly is ~7% and the sum natural occurrence for the charged residues is ~23%.

Figure 6: A model for the evolutionary origin of the NPC. A primitive coating complex (bottom, purple) evolved into numerous vesicle coating complexes (pink) and a simpler pre-NPC, which through duplication and divergence of its constituents produced

a complex and elaborate NPC in the LCEA. The composition and architecture of the contemporary NPC throughout the Eukaryota is largely conserved, with species-specific adaptations arising primarily by divergent evolution. The inferred degrees of conservation of the indicated different architectural elements of the trypanosome, yeast and vertebrate NPC (with vertebrate set as the standard) is shown in shades of blue, based on the analysis presented here.

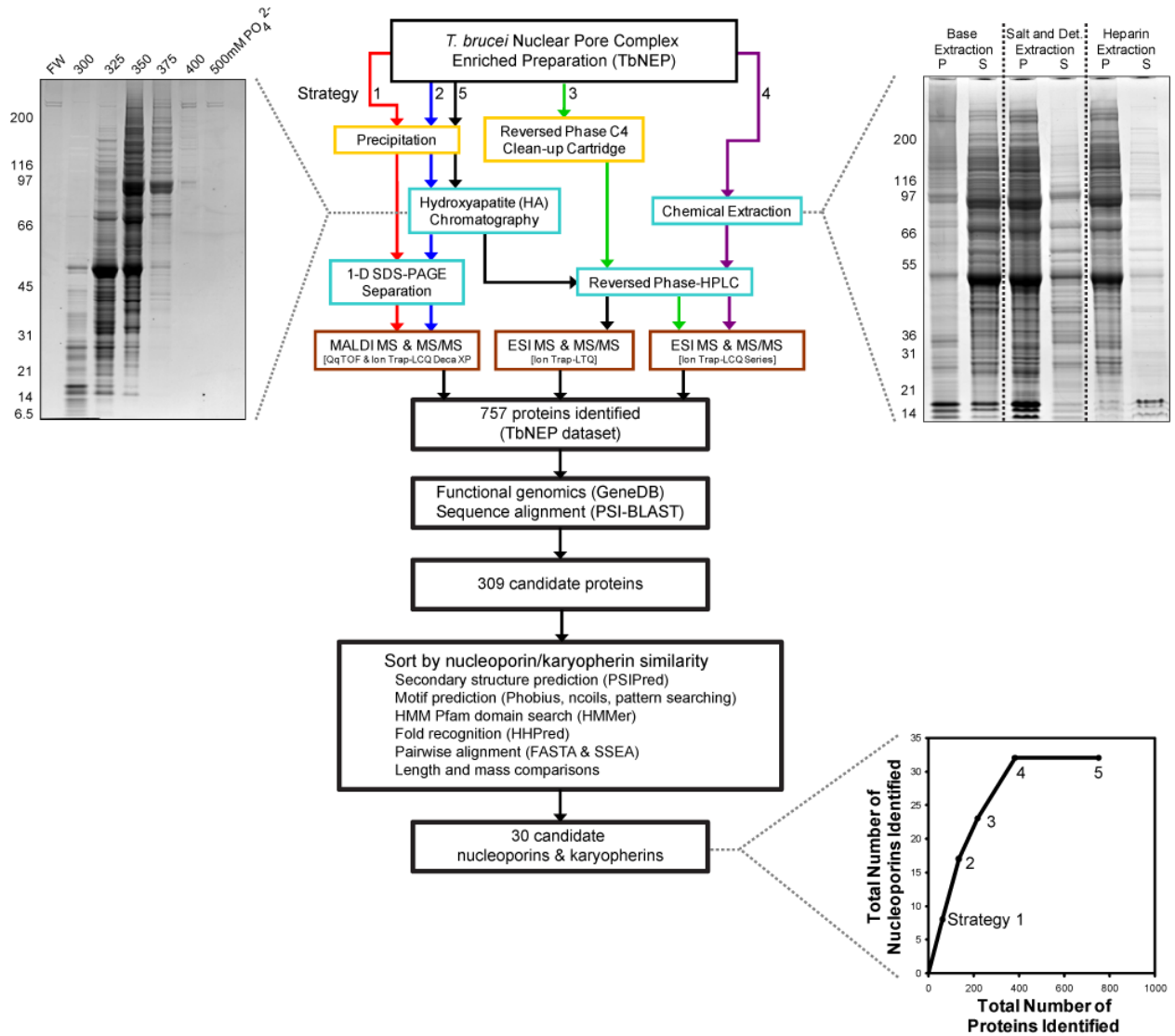


Fig. 1

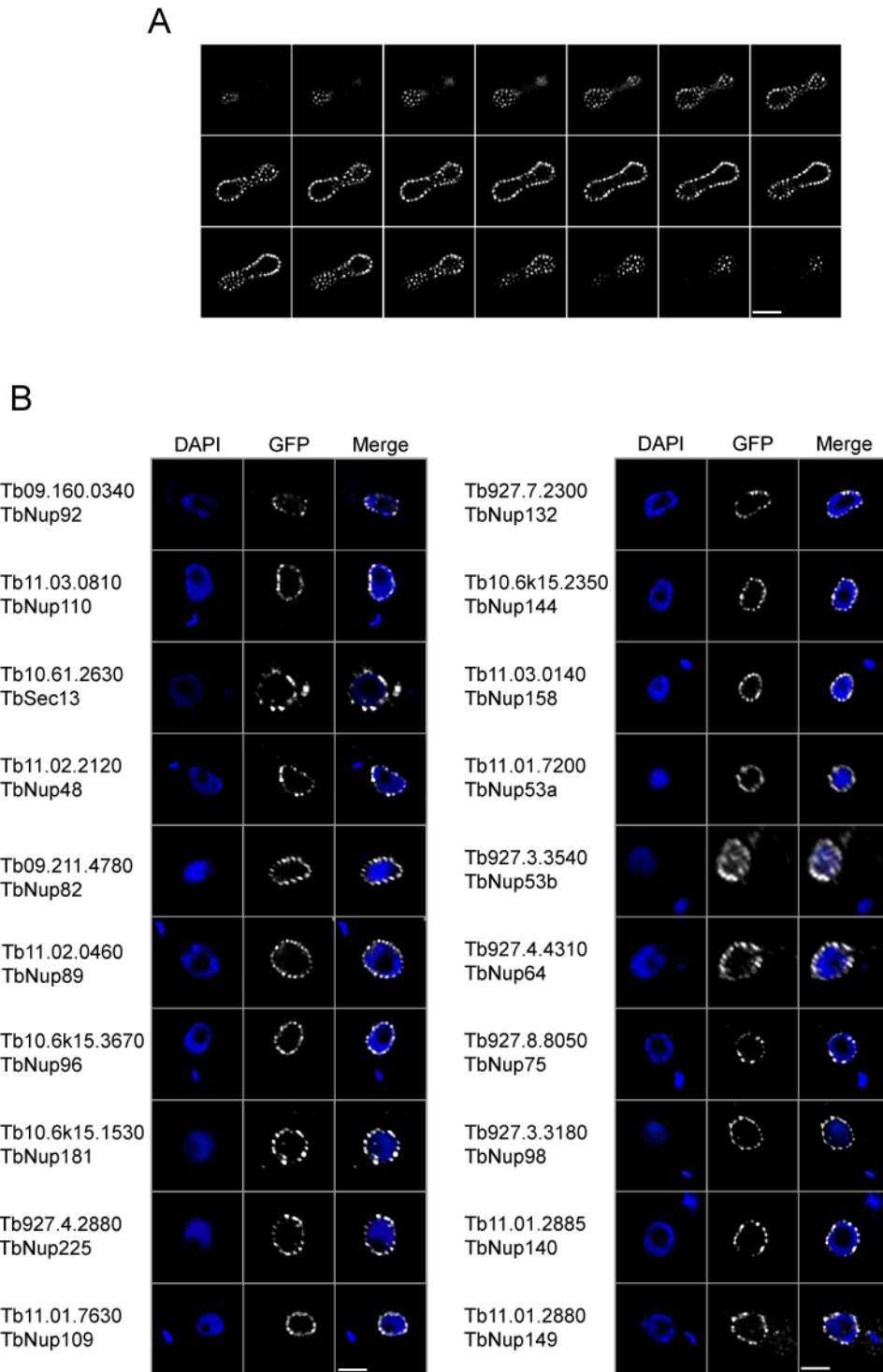


Fig. 2

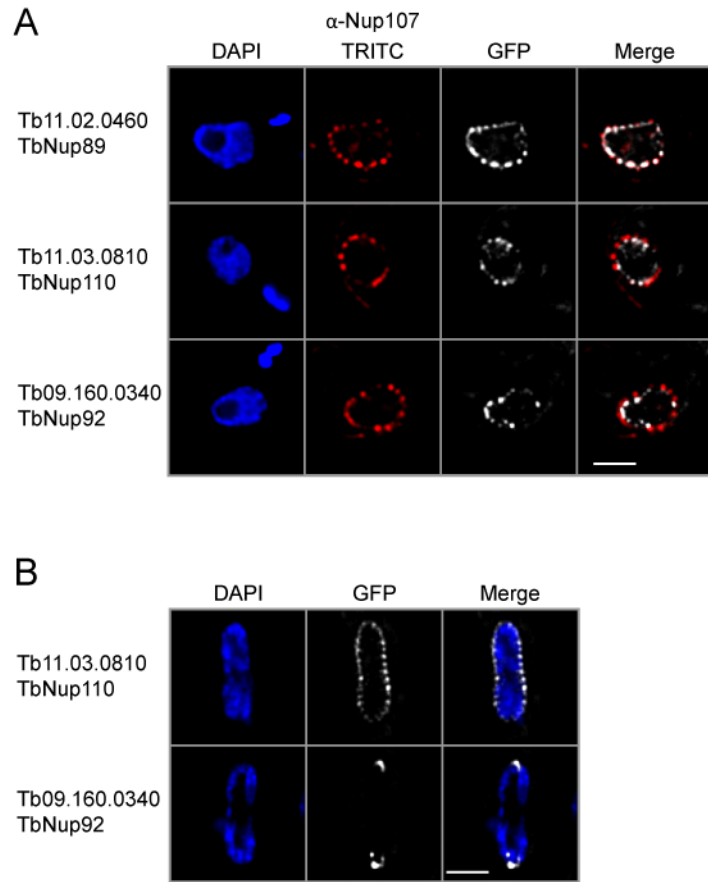


Fig.3

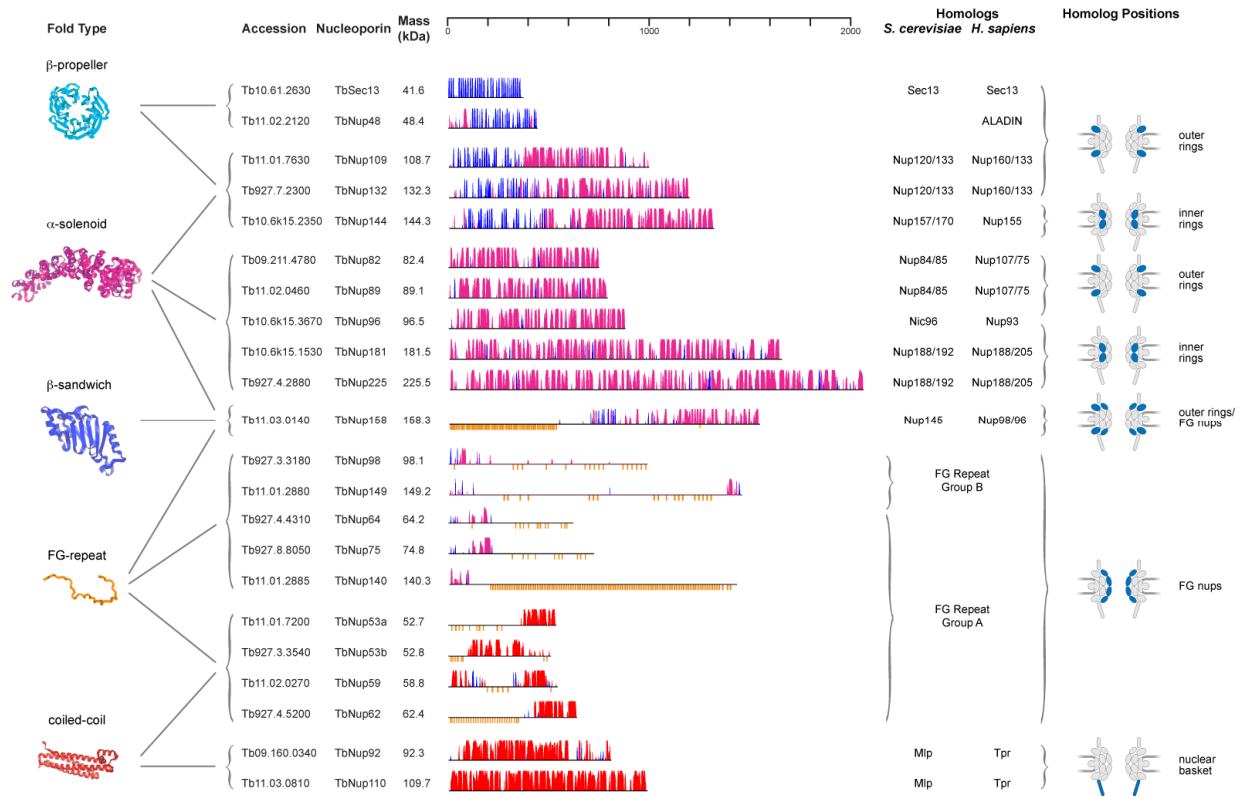


Fig. 4

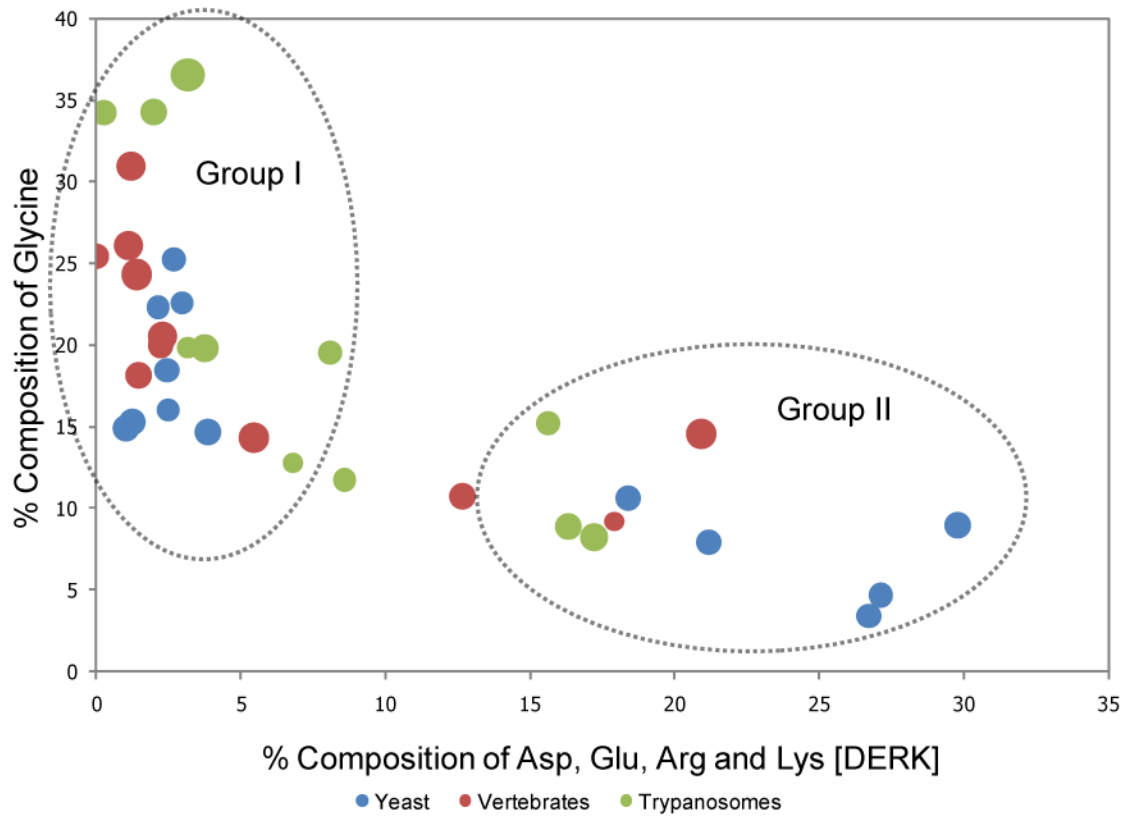


Fig. 5

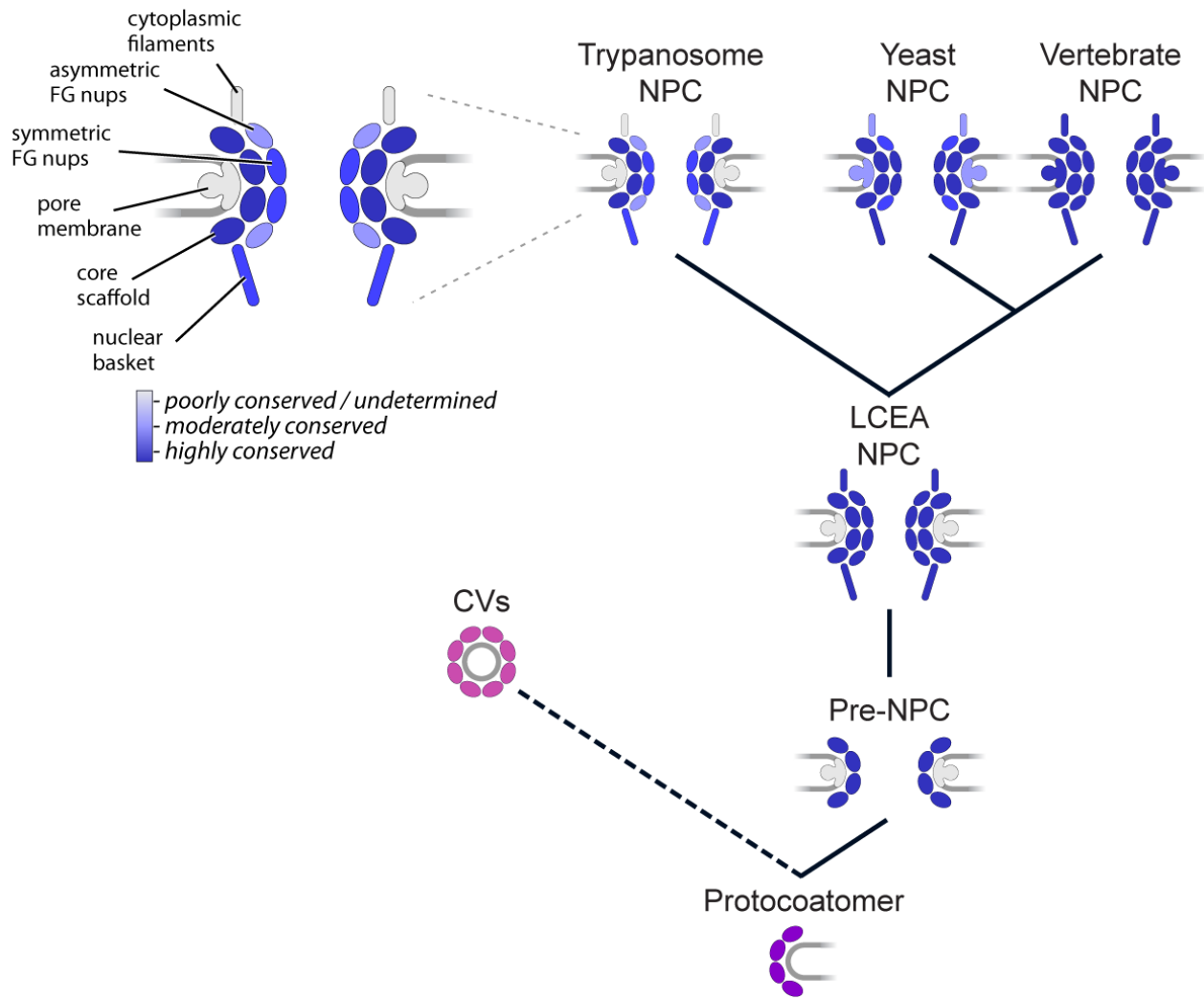


Fig. 6

Table 1: Putative TbNPC Associated proteins. (a) The residue boundaries of the domains are listed along with the domain identifier: CC, coiled coil; FG, FG repeat. The most abundant FG repeat motif is listed within brackets.

Accession Number	Annotation	Mass (kDa)	log(e)	# of unique identified peptides	Sequence Coverage (%)	Category	Domains or Fold Type (a)	GFP localized?
Tb09.160.0340	TbMlp-2	92.3	-2.2	3	6.2	Mlp	CC: 88-200, 206-283, 294-368, 416-596	SPB during anaphase
Tb11.03.0810	TbMlp-1	109.6	-23.8	13	19.5	Mlp	CC: 292-336, 383-426, 436-496, 638-671, 689-748, 852-881, 884-974	Yes
Tb10.61.2630	TbSec13	41.6	-14.5	4	12.0	Nup	Beta Propeller	Yes
Tb11.02.2120	TbNup48	48.4	-15.9	5	14.1	Nup	Beta Propeller	Yes
Tb09.211.4780	TbNup82	82.3	-35.0	16	30.4	Nup	Alpha Solenoid	Yes
Tb11.02.0460	TbNup89	89	-52.8	19	32.6	Nup	Alpha Solenoid	Yes
Tb10.6k15.3670	TbNup96	96.4	-74.6	23	39.9	Nup	Alpha Solenoid	Yes
Tb11.01.7630	TbNup109	108.6	-21.9	9	10.8	Nup	Beta Propeller Alpha Solenoid	Yes
Tb927.7.2300	TbNup132	132.2	-30.8	14	14.6	Nup	Beta Propeller Alpha Solenoid	Yes
Tb10.6k15.2350	TbNup144	144.2	-70.9	27	30.5	Nup	Beta Propeller Alpha Solenoid	Yes
Tb10.6k15.1530	TbNup181	181.4	-15.7	7	6.7	Nup	Alpha Solenoid	Yes
Tb927.4.2880	TbNup225	225.4	-35.9	20	19.5	Nup	Alpha Solenoid	Yes
Tb11.01.7200	TbNup53a	52.7	-27.6	8	31.5	Nup FG	CC: 407-443; FG (GFG): 16-263	Yes
Tb927.3.3540	TbNup53b	52.8	-36.0	9	34.2	Nup FG	CC: 159-194, 248-262, 364-378; FG (GFG): 10-72	Yes
Tb11.02.0270	TbNup59	58.7	-24.3	6	14.4	Nup FG	CC: 452-509, 617-638; FG (FGFG): 194-299	Not Tagged
Tb927.4.5200	TbNup62	62.4	-26.0	9	29.9	Nup FG	FG (GGFGA): 8-349; CC: 453-486, 493-521	Not Tagged
Tb927.4.4310	TbNup64	64.1	-52.6	13	27.7	Nup FG	CC: 149-228; FG (FSFG): 331-583	Yes
Tb927.8.8050	TbNup75	74.7	-3.2	2	4.0	Nup FG	CC: 150-237; FG (FSFG): 317-684	Yes
Tb927.3.3180	TbNup98	98	-129.9	20	27.6	Nup FG	FG (FSFG): 321-986	Yes
Tb11.01.2885	TbNup140	140.2	-20.2	9	17.6	Nup FG	FG ([A/V]FGQ): 209-1432	Yes
Tb11.01.2880	TbNup149	149.1	-2.9	2	2.9	Nup FG	FG (VFGT): 267-388, 1007-1288	Yes
Tb11.03.0140	TbNup158	158.2	-99.7	33	35.7	Nup FG	FG (GGFGQ): 5-550; Beta Sandwich: 713-851; Alpha Solenoid	Yes
Tb927.7.5760	TbNTF2	15.8	-2.7	3	45.9	Transport Factor		Not Tagged
Tb11.02.0870	Ran-binding protein 1	17.6	-13.0	3	24.8	Transport Factor		Not Tagged
Tb927.3.1120	TbRTB2	24.3	-109.9	23	83.4	Transport Factor		Not Tagged
Tb09.160.2360	TbGLE2	38.3	-8.4	4	14.6	Transport Factor	Beta Propeller	Not Tagged
Tb927.6.2640	TbKap60	58	-18.6	6	18.3	Transport Factor		Not Tagged
Tb10.70.4720	TbKap95	95	-8.5	4	9.5	Transport Factor		Not Tagged
Tb10.6k15.3020	TbKap104	103.8	-2.5	2	5.4	Transport Factor	transportin2 - like	Not Tagged
Tb11.01.7010	TbKap123	117.8	-16.6	4	7.9	Transport Factor		Not Tagged